IEEE Photonics Journal
An IEEE Photonics Society Publication

Open Access

Unidirectional Optical Transmission in a Single-Layer Metallic Grating Consisting of Cambered Resonators

Volume 10, Number 4, August 2018

Pengwei Xu
Mingsi Zhang
Zongqiang Chen
Jiwei Qi
Jing Chen
Jun Qian
Yudong Li
Qian Sun
Jingjun Xu

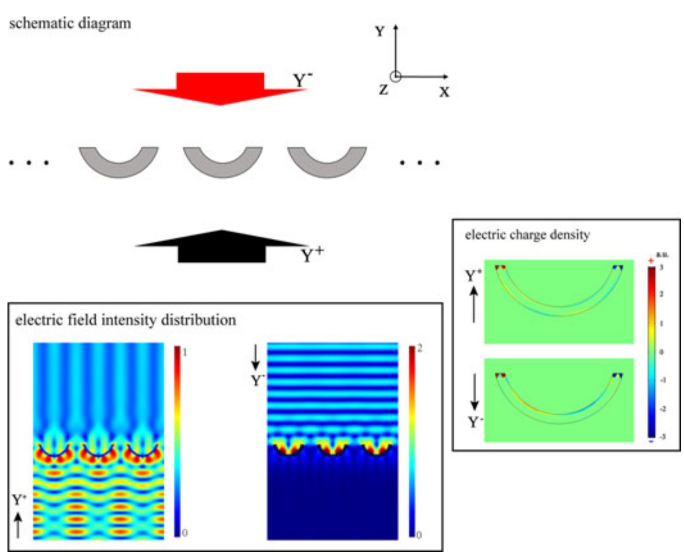

DOI: 10.1109/JPHOT.2018.2850321
1943-0655

Unidirectional Optical Transmission in a Single-Layer Metallic Grating Consisting of Cambered Resonators

Pengwei Xu,[1] **Mingsi Zhang**,[1] **Zongqiang Chen**,[1] **Jiwei Qi**,[1,2] **Jing Chen**,[1] **Jun Qian**,[1] **Yudong Li**,[1,2] **Qian Sun**,[1,2,3] **and Jingjun Xu**[1,2]

[1]MOE Key Laboratory of Weak Light Nonlinear Photonics, Tianjin Key Laboratory of Photonics Materials and Technology of Information Science, School of Physics, Nankai University, Tianjin 300071, China
[2]Collaborative Innovation Center of Extreme Optics, Shanxi University, Taiyuan 030006, China
[3]Sino-Canada R&D Center on Water and Environmental Safety, Nankai University, Tianjin 300071, China

DOI:10.1109/JPHOT.2018.2850321

Manuscript received March 15, 2018; revised June 10, 2018; accepted June 21, 2018. Date of publication July 4, 2018; date of current version July 17, 2018. Corresponding author: Qian Sun.

Abstract: In order to realize unidirectional optical transmission (UOT), a single-layer metallic grating (SMG) consisting of cambered resonators (CRs) is proposed. Numerical simulation results show that the transmittance contrast ratio of the SMG can reach about 5000 with a high unidirectional transmittance of 39%. UOT results from diffraction enhancement or suppression in transmission direction. Diffraction is manipulated by the interference of electromagnetic radiation from local surface plasmons on CRs. Our single-layer structure has sub-100 nm thickness and can be used in ultracompact optical devices to manipulate light transmission.

Index Terms: Surface plasmons, unidirectional transmission, metallic grating.

1. Introduction

Unidirectional optical transmission (UOT) [1] means that light can transmit in one direction and is blocked in the reverse direction. The roles of UOT devices in photonic circuits are similar to that of electronic diodes in electronic circuits. UOT can be classified into two types. One runs counter to Lorentz reciprocity and the other follows reciprocity theory [2]. In the first type, the use of Magneto-optical [3], [4], liquid crystals [5], [6] or time-dependent [7] media inevitably comes up with an external either magnetic or electric field, which usually requires a precise and reliable control over the position, magnitude and direction of the field. Similarly, nonlinear media [8], [9] calls for high intensity. The second type is made of isotropic and linear materials and takes photonic crystals [10]–[12], gratings [13]–[15], and grating-photonic crystal [16], [17] as universal structures.

In the recent years, metallic micro/nano structures are popular and widely studied because surface plasmons (SPs) [18], i.e., oscillating electrons patterns, of metal allow for manipulating electromagnetic wave in nano-scale. Such as the insertion of metal slab in dielectric gratings [19], [20], asymmetric dual-gratings-structure [21], [22], metamaterials [23], [24], metallic slots [25] and slit [26], many novel structures are gradually emerging and used to realize UOT. Among them,

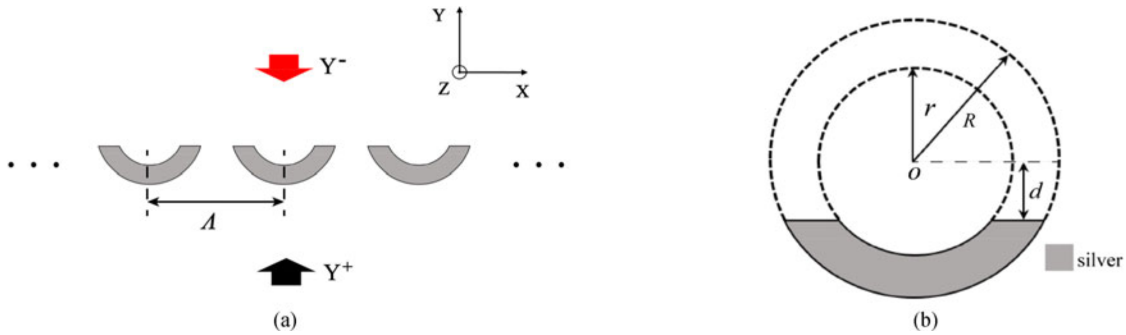

Fig. 1. Schematic of the (a) SMG and the geometry of a single (b) CR.

most structures are compounded of multiple layers and need special alignment of different layers. Single-layer structure is rare and the UOT performance of a single metal film [27] needs to be improved.

In this paper, a single-layer metallic grating (SMG), consisting of periodic cambered resonators (CRs), is proposed to realize UOT. The simulation results show that the transmittance contrast ratio between two contrary incident directions can reach about 5000, with a high unidirectional transmittance of 39%. It suggests that the SMG is a good component in UOT devices. In our work, it is demonstrated that the UOT results from enhanced or suppressed diffraction in transmission direction of the SMG. The difference in diffraction intensities is caused by the interference of electromagnetic radiation from local surface plasmons (LSPs) on CRs.

2. Structure and Parameters Definitions

Fig. 1(a) is the diagram of the proposed SMG, composed of periodic CRs. Fig. 1(b) illustrates the geometry of a CR. The CR is minor arc as a portion of a concentric ring. The inner and outer radii are denoted as R and r, respectively. The separation between the flat kerfs and the center of the ring is signed by d. The period, i.e., the grating constant of the SMG, is denoted by Λ. The CRs are made of silver and supposed standing freely in the air. The frequency-dependent complex relative permittivity of silver is characterized by the Drude model [28]:

$$\varepsilon(\omega) = 1 - \frac{\omega_p^2}{\omega^2 + i\omega\gamma}. \tag{1}$$

Here, the plasma resonance frequency ω_p is 1.37×10^{16} rad/s and the electrons characteristic collision frequency γ is 3.21×10^{13} Hz. ω represents the angular frequency of the incident beam. The values of ω_p and γ are chosen to fit with the experimental data of Johnson and Christy [29].

The incident light is transverse magnetic (TM) plan wave. Y^+ (Y^-) represents the incident light along positive (negative) direction of y-axis. The transmittance is

$$T = \frac{P_0}{P_i}, \tag{2}$$

where P_0 is the output power and P_i is incident power. T^+ and T^- represent the transmittance of a SMG for Y^+ and Y^-, respectively. The transmittance contrast ratio η is used to describe the UOT performance and defined as:

$$\eta = \frac{T^+}{T^-}. \tag{3}$$

In our UOT research, we seek for the cases of $\eta \gg 1$ or $\eta \ll 1$, while T^+ or T^- has a relatively large value.

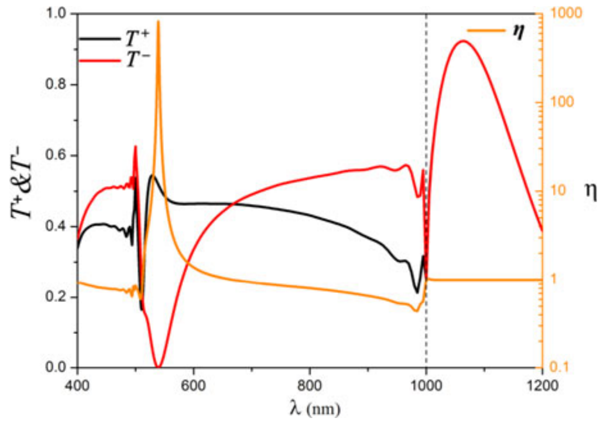

Fig. 2. T^+, T^- and η of a SMG with $r = 300$ nm, $R = 350$ nm, $d = 80$ nm and $\Lambda = 1000$ nm.

The proposed SMG is numerically simulated by COMSOL Multiphysics, which can accurately calculate the electromagnetic interaction between light and matter based on Finite Element Method [30].

3. Numerical Simulation Results and Analyses

Fig. 2 shows T^+, T^- and η of a SMG with $r = 300$ nm, $R = 350$ nm, $d = 80$ nm and $\Lambda = 1000$ nm. A critical wavelength λ_c is marked by a vertical black dash line and it equals the granting constant Λ. The transmission spectrum can be separated into two regions according to λ_0. When $\lambda > \lambda_c$, $T^+ = T^-$ and thus $\eta = 1$. By contrast, when $\lambda \leq \lambda_c$, $T^+ \neq T^-$ and η changes non-monotonously with the decrease of λ. η reaches the minimum 0.4406 at 985 nm due to $T^+ = 0.21$ and $T^- = 0.48$, and reaches its maximum 819.7 at 539 nm while $T^+ = 0.52$ and $T^- = 6.3 \times 10^{-4}$. So, the SMG realizes perfect UOT for the case of $\eta \gg 1$. In the following discussion, λ is fixed between 500 nm to 650 nm.

The diffraction of a grating is produced by the interference between grating cells and follows

$$\mathrm{m}\lambda_0 = \Lambda(n_o \sin\theta_\mathrm{m} - n_i \sin\theta_i), \tag{4}$$

where $\mathrm{m} = 0, \pm 1, \pm 2, \ldots, \lambda_0$ is free-space wavelength. $\mathrm{n_0}$ and $\mathrm{n_i}$ are the refractive indexes at output- and input-side of light, respectively. θ_i is incidence angle and θ_m is angle of m-order diffraction. For our simulation, Eq. (4) can be simplified as

$$\mathrm{m}\lambda = \Lambda \sin\theta_\mathrm{m}, \tag{5}$$

because of $\mathrm{n_0} = \mathrm{n_i} = 1$, $\lambda = \lambda_0$ and $\theta_i = 0$. Eq. (5) shows θ_m is dependent on the period of grating cells. However, the efficiency of m-order diffraction is dependent on concrete size and shape of the resonator in a grating cell.

Actually, it is the non-reciprocal diffraction that leads to the UOT of the SMG. Transmittance, in Eq. (2), is calculated by integrating the Poynting vector on an observation line in our simulation and the energies of forward-propagating diffraction waves are included in. The diffraction intensities in transmittance are further calculated using diffraction ports. Fig. 3 shows the diffraction intensities of a SMG with the same geometry parameters in Fig. 2. When λ is between 500 nm and 650 nm, 0, $+1$ and -1 order diffractions exist. 0-order transmission is represented by T_0^+ for Y^+ and T_0^- for Y^-. $+1$ and -1 order diffraction intensities are equal because of the vertically incidence and are represented by a common symbol T_1^+ for Y^+ (T_1^- for Y^-). In Fig. 3, $T_0^+ = T_0^-$ at any λ, but $T_1^+ \neq T_1^-$ because of non-reciprocal diffraction. The transmittance calculated by integral is the sum of forward diffractions. Therefore, the expansion of Eq. (3) is $\eta = (T_0^+ + 2T_1^+)/(T_0^- + 2T_1^-)$. The necessary condition for $\eta \gg 1$ is $T_1^+ >> T_1^-$ while $T_0^+ = T_0^- \approx 0$. In Fig. 3, when λ is 539 nm, $T_0^+ = T_0^- \approx 0$ implying the incident light is totally reflected backward and absorbed by CRs.

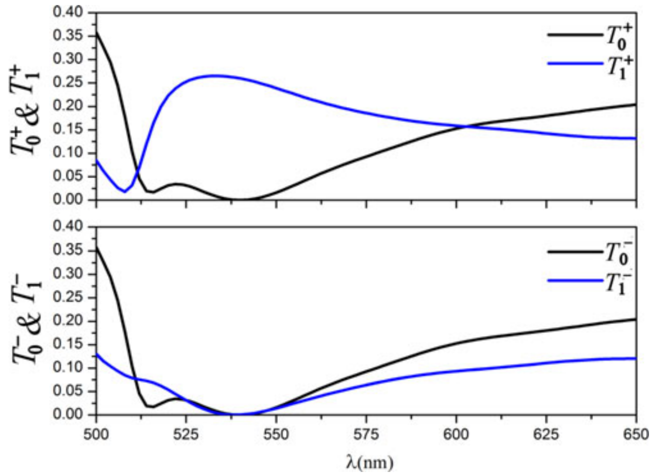

Fig. 3. The intensities of 0 and 1 order diffraction for Y^+ and Y^-. Here, $r = 300$ nm, $R = 350$ nm, $d =$ 80 nm and $\Lambda = 1000$ nm.

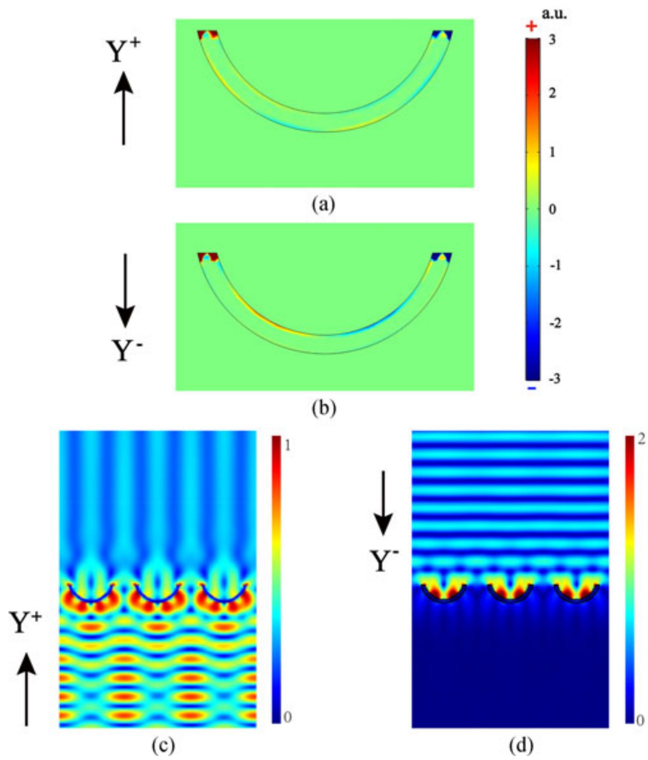

Fig. 4. The charge distributions on a CR and electric field intensity distributions around the SMG. (a) and (c) are for Y^+. (b) and (d) are for Y^-. Here, λ is 539 nm, $r = 300$ nm, $R = 350$ nm and $\Lambda = 1000$ nm, and $d = 80$ nm.

Meanwhile, $T_1^+ = 0.26$ and $T_1^- = 2.7 \times 10^{-4}$. It is corresponding to $T^+ = 0.52$ and $T^- = 6.3 \times 10^{-4}$ at $\lambda = 539$ nm in Fig. 2.

The SMG periodically modulates the amplitude and phase of the incident light and splits the incident wave into diffraction waves traveling forward. LSP resonances on CRs lead to field amplification in the near-field zone and further influence the interference between adjacent CRs which

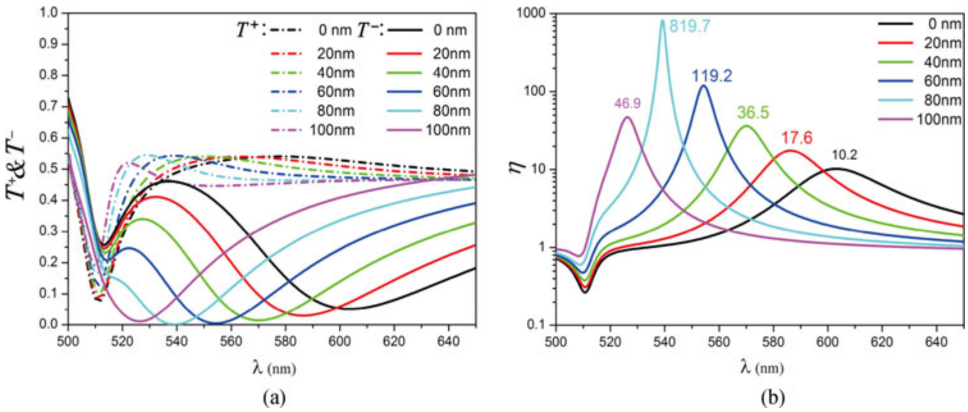

Fig. 5. The influence of d on (a) T^+, T^- and (b) η. Here, $r = 300$ nm, $R = 350$ nm, $\Lambda = 1000$ nm and $d = 0$ nm, 20 nm, 40 nm, 60 nm, 80 nm and 100 nm, respectively.

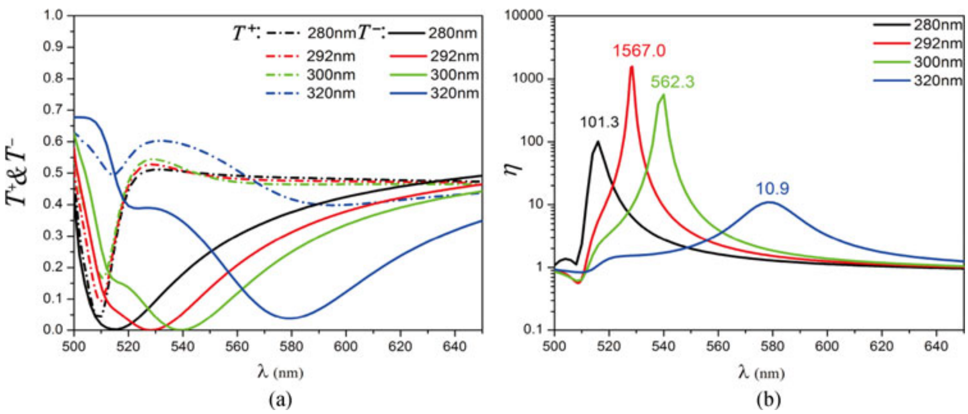

Fig. 6. The influence of r on (a) T^+, T^- and (b) η. Here, $R = 350$ nm, $\Lambda = 1000$ nm $d = 80$ nm and $r =$ 280 nm, 292 nm, 300 nm and 320 nm, separately.

plays an important role for light transmission. Fig. 4(a) and (b) show the charge distributions on a CR at $\lambda = 539$ nm for Y^+ and Y^-, respectively. The corresponding electric field intensity distributions are shown in Fig. 4(c) and (d). The LSPs are produced on CRs through the interaction between CRs and incident light. Charge distributions show that the excitations efficiency of LSP for the same surface of a CR are different for Y^+ and Y^-. The electric field distributions indicate that the interference of electromagnetic radiation from LSPs on the CRs is important for light transmission. For Y^+, the inner arc and two flat kerfs of CRs act as the exit surface. LSPs at the exit surface are obvious in Fig. 4(a) and the electromagnetic radiation from LSPs on the exit surface leads to much light is diffracted as ± 1 order which explain for the periodic intensity distributions along forward direction in Fig. 4(c). For Y^-, the outer arc of the CR acts as the exit surface and LSPs existing on the outer arc are weak seen from Fig. 4(b). Contrarily, LSPs on the entrance surface (the inner arc and two flat kerfs) are strong, leading to high reflectance and low transmittance. So, it is the peculiar geometrical shape and the radiation of LSPs of CRs that modulates the diffraction intensity and result in UOT of the SMG. The interference of electromagnetic radiation from LSPs that making 0 order transmission suppressed and ± 1 order diffractions enhanced or suppressed.

CRs surface topography influences the LSPs resonances and modulates the interference of electromagnetic radiation from LSPs. The difference between upper and lower surface topography of CRs makes the electromagnetic radiation interference different, leading to UOT. The influence of geometric parameter d on UOT is investigated. We keep $r = 300$ nm, $R = 350$ nm and $\Lambda = 1000$ nm. T^+, T^-, and η are displayed in Fig. 5 for $d = 0$ nm, 20 nm, 40 nm, 60 nm, 80 nm and

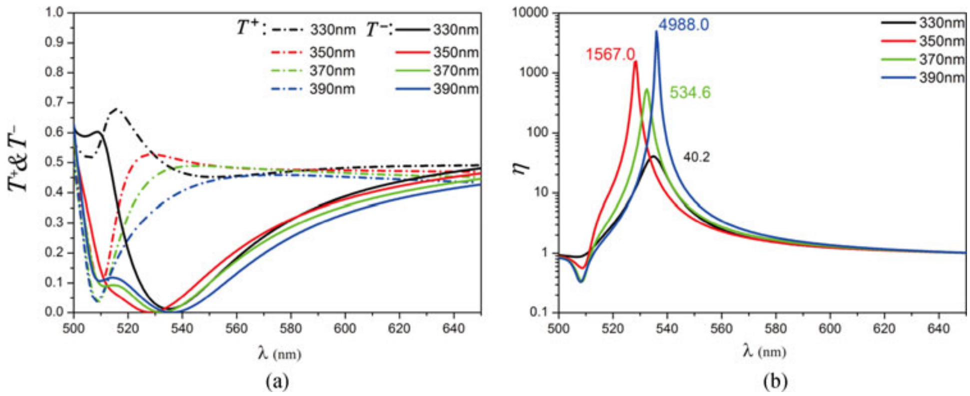

Fig. 7. The influence of R on (a) T^+, T^- and (b) η. Here, $r = 292$ nm, $\Lambda = 1000$ nm, $d = 80$ nm and $R = 330$ nm, 350 nm, 370 nm and 390 nm, separately.

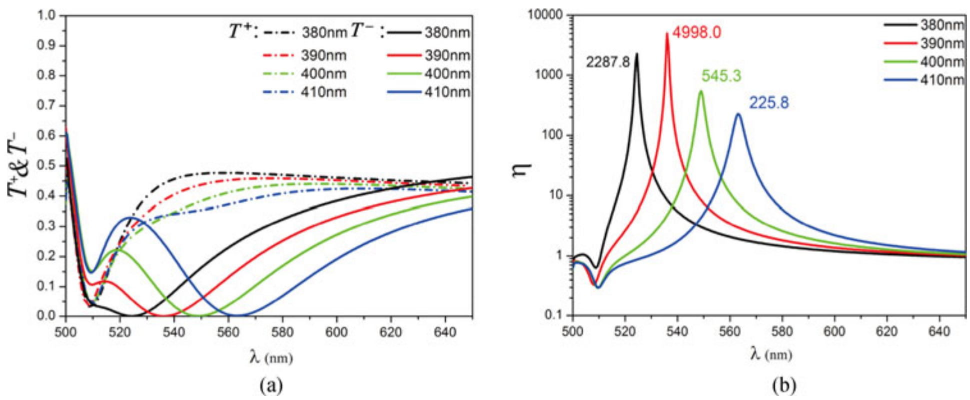

Fig. 8. When R-$r = 98$ nm, the influence of R on (a) T^+, T^- and (b) η. Here, $\Lambda = 1000$ nm, $d = 80$ nm and $R = 380$ nm, 390 nm, 400 nm and 410 nm, respectively.

100 nm. Fig. 5(a) shows d has a significant influence on T^-. A dip in T^- curves has obvious blue shift along with the increase of d. The blue shift of the dip in T^- results to blue shift of the peak in η. In Fig. 5(b), the maximum of η increases non-monotonically along with the increase of d and is about 820 at $\lambda = 539$ nm when d is 80 nm.

The influence of r on UOT of a SMG with $R = 350$ nm, $\Lambda = 1000$ nm and $d = 80$ nm is shown in Fig. 6. T^- changes greatly with r. In Fig. 6(a), the dip in T^- curves has obvious red shift along with the increase of r. By comparing Figs. 6(a) with 5(a), the influences of increasing r and decreasing d on T^- are similar. The red shift of the dip in T^- curves, shown in Fig. 6(a), results to red shift of the peak of η, shown in Fig. 6(b). The maximum of η reaches 1567.0 at $\lambda = 529$ nm when r is 292 nm while T^- reaches the minimum 3.4×10^{-14}.

Fig. 7 shows the influence of R on the performance of a SMG with $r = 292$ nm, $\Lambda = 1000$ nm and $d = 80$ nm. In Fig. 7(a), the wavelength of the dip in T^- curves has a small change around 530 nm and T^+ has an obvious change along with the increase of R. The influences of R on the dip position in T^- curves is much less than the influence of d and r. T^+ depends more on R and d than r. The dip position in T^- curves determines the peak position of η. In Fig. 7(b), the maximum of η reaches about 5000 due to $T^- = 0.77 \times 10^{-4}$ and $T^+ = 0.39$, at $\lambda = 536$ nm when R is 390 nm and R-$r =$ 98 nm.

When R-$r = 98$ nm, the influence of R on the UOT of a SMG with $\Lambda = 1000$ nm and $d = 80$ nm is shown in Fig. 8. Fig. 8(a) shows that wavelength of the dip in T^- curves red shifts and the maximum of T^+ decreases along with the increase of *R*. In Fig. 8(b), the peak position of η red shifts with *R* the increases. However, the maximum of η doesn't gets larger than 5000. Seen from Figs. 5–8, the size of inner arc and the wavelength of the dip in T^- curves have positive correlation, e.g., LSPs resonance on inner arc of CRs count for UOT This confirms Fig. 4(b). Our investigation shows that the UOT of a SMG results from non-reciprocal diffraction and non-reciprocal diffraction efficiency is influenced by the structure size of a CR. In essence, the structure size influences LSPs resonance on CRs.

4. Conclusions

In this paper, a single-layer metallic grating consisting of cambered resonators is proposed to realize unidirectional optical transmission. It is the interference of electromagnetic radiation from local surface plasmons on the cambered resonators that makes diffraction enhanced or suppressed, leading to unidirectional optical transmission. In our research, the transmittance contrast ratio of this single-layer metallic grating can reach about 5000 with a high unidirectional transmittance of 39%. The characteristic of single layer and the good performance of unidirectional optical transmission indicate that the single-layer metallic grating is a potential candidate for unidirectional optical transmission devices.

Acknowledgment

The authors would like to acknowledge the financial support from National Natural Science Foundation of China (11504185, 61178004), Fundamental Research Funds for the Central Universities, and Natural Science Foundation of Tianjin (06TXTJJC13500) and Science and Technology Commission of Tianjin Binhai New Area (BHXQKJXM-PT-ZJSHJ-2017003).

References

[1] P. N. Melentiev, A. E. Afanasiev, A. S. Kalmykov, and V. I. Balykin, "Light transmission asymmetry and optical diode," *Eur. Phys. J. D*, vol. 71, no. 6, pp. 1–5, 2017, Art. no. 152.
[2] D. Jalas *et al.*, "What is – and what is not – an optical isolator," *Nature Photon.*, vol. 7, no. 8, pp. 579–582, 2013.
[3] P. Pintus, M. C. Tien, and J. E. Bowers, "Design of magneto-optical ring isolator on SOI based on the finite-element method," *IEEE Photon. Technol. Lett.*, vol. 23, no. 22, pp. 1670–1672, Nov. 2011.
[4] M. C. Tien, T. Mizumoto, P. Pintus, H. Kromer, and J. E. Bowers, "Silicon ring isolators with bonded nonreciprocal magneto-optic garnets," *Opt. Exp.*, vol. 19, no. 12, pp. 11740–11745, 2011.
[5] A. El-Metwally, N. Areed, M. Hameed, and S. Obayya, "Reconfigurable unidirectional photonic crystal using liquid crystal layer," *IEEE Photon. J.*, vol. 9, no. 1, Feb. 2017, Art. no. 4500209.
[6] M. H. Song *et al.*, "Simple electro-tunable optical diode using photonic and anisotropic liquid crystal films," *Thin Solid Films*, vol. 509, no. 1–2, pp. 49–52, 2006.
[7] D. L. Sounas and A. Alù, "Non-reciprocal photonics based on time modulation," *Nature Photon.*, vol. 11, no. 12, pp. 774–783, 2017.
[8] C. Y. Wang *et al.*, "All-optical transistor-and diode-action and logic gates based on anisotropic nonlinear responsive liquid crystal," *Sci. Rep.*, vol. 6, no. 1, 2016, Art. no. 30873.
[9] L. Fan *et al.*, "An all-silicon passive optical diode," *Science*, vol. 335, no. 6067, pp. 447–450, 2012.
[10] D. Liu, S. Hu, and Y. Gao, "One-way optical transmission in silicon photonic crystal heterojunction with circular and square scatterers," *Phys. Lett. A*, vol. 381, no. 25–26, pp. 2131–2135, 2017.
[11] A. E. Serebryannikov, "One-way diffraction effects in photonic crystal gratings made of isotropic materials," *Phys. Rev. B, Condens. Matter*, vol. 80, no. 15, 2009, Art. no. 155117.
[12] A. E. Serebryannikov, A. O. Cakmak, and E. Ozbay, "Multichannel optical diode with unidirectional diffraction relevant total transmission," *Opt. Exp.*, vol. 20, no. 14, pp. 14980–14990, 2012.
[13] C. Zeng, W. M. Ye, and X. D. Yuan, "Unidirectional transmission realized by two nonparallel gratings made of isotropic media," *Opt. Lett.*, vol. 36, no. 15, pp. 2842–2844, 2011.
[14] W. M. Ye, X. D. Yuan, C. C. Guo, and C. Zen, "Unidirectional transmission in non-symmetric gratings made of isotropic material," *Opt. Exp.*, vol. 18, no. 8, pp. 7590–7595, 2010.
[15] Y. Xu, L. Feng, M. Lu, and Y. Chen, "Unidirectional transmission based on a passive PT symmetric grating with a nonlinear silicon distributed Bragg reflector cavity," *IEEE Photon. J.*, vol. 6, no. 1, Feb. 2014, Art. no. 0600507.
[16] Ł. Zinkiewicz, J. Haberko, and P. Wasylczyk, "Highly asymmetric near infrared light transmission in an all-dielectric grating-on-mirror photonic structure," *Opt. Exp.*, vol. 23, no. 4, pp. 4206–4211, 2015.
[17] Y. Zhang, Q. Kan, and G. P. Wang, "One-way optical transmission in silicon grating-photonic crystal structures," *Opt. Lett.*, vol. 39, no. 16, pp. 4934–4937, 2014.

[18] M. L. Brongersma and P. G. Kik, *Surface Plasmon Nanophotonics*. New York, NY, USA: Springer, 2007.
[19] A. E. Serebryannikov and E. Ozbay, "Isolation and one-way effects in diffraction on dielectric gratings with plasmonic inserts," *Opt. Exp.*, vol. 17, no. 1, pp. 278–292, 2009.
[20] A. E. Serebryannikov and E. Ozbay, "Unidirectional transmission in non-symmetric gratings containing metallic layers," *Opt. Exp.*, vol. 17, no. 16, pp. 13335–13345, 2009.
[21] Z. H. Zhu *et al.*, "One-way transmission of linearly polarized light in plasmonic subwavelength metallic grating cascaded with dielectric grating," *Opt. Lett.*, vol. 37, no. 19, pp. 4008–4010, 2012.
[22] J. Xu *et al.*, "Unidirectional optical transmission in dual-metal gratings in the absence of anisotropic and nonlinear materials," *Opt. Lett.*, vol. 36, no. 10, pp. 1905–1907, 2011.
[23] C. Menzel *et al.*, "Asymmetric transmission of linearly polarized light at optical metamaterials," *Phys. Rev. Lett.*, vol. 104, no. 25, 2010, Art. no. 253902.
[24] Z. Li *et al.*, "Broadband diodelike asymmetric transmission of linearly polarized light in ultrathin hybrid metamaterial," *Appl. Phys. Lett.*, vol. 105, no. 20, 2014, Art. no. 201103.
[25] X. Hu, Y. Zhang, X. Xu, and Q. Gong, "Nanoscale surface plasmon all-optical diode based on plasmonic slot waveguides," *Plasmonics*, vol. 6, no. 4, pp. 619–624, 2011.
[26] H. Hu *et al.*, "Unidirectional coupling of surface plasmon polaritons by a single slit on a metal substrate," *IEEE Photon. Technol. Lett.*, vol. 28, no. 21, pp. 2395–2398, Nov. 2016.
[27] N. Peng and W. She, "Asymmetric optical transmission through periodic arrays of cone air holes in a metal film," *Opt. Exp.*, vol. 22, no. 23, pp. 28452–28458, 2014.
[28] J. A. Dionne, L. A. Sweatlock, H. A. Atwater, and A. Polman, "Planar metal plasmon waveguides: Frequency-dependent dispersion, propagation, localization, and loss beyond the free electron model," *Phys. Rev. B*, vol. 72, no. 7, 2005, Art. no. 075405.
[29] P. B. Johnson and R. W. Christy, "Optical constants of the noble metals," *Phys. Rev. B*, vol. 6, no. 12, pp. 4370–4379, 1972.
[30] J. Whiteley, *Finite Element Methods*. Cham, Switzerland: Springer, 2017.